Limnol. Oceanogr., 57(2), 2012, 607–618

doi:10.4319/lo.2012.57.2.0607

Effects of CO_2 and their modulation by light in the life-cycle stages of the coccolithophore *Emiliania huxleyi*

Sebastian D. Rokitta* and Björn Rost

Alfred Wegener Institute for Polar and Marine Research, Bremerhaven, Germany

Abstract

The effects of ocean acidification on the life-cycle stages of the coccolithophore *Emiliania huxleyi* and their modulation by light were examined. Calcifying diploid and noncalcifying haploid cells (Roscoff culture collection strains 1216 and 1217) were acclimated to present-day and elevated CO_2 partial pressures (P_{CO_2}; 38.5 vs. 101.3 Pa, i.e., 380 vs. 1000 μatm) under low and high light (50 vs. 300 μmol photons m^{-2} s^{-1}). Growth rates as well as cellular quotas and production rates of C and N were measured. Sources of inorganic C for biomass buildup were determined using a ^{14}C disequilibrium assay. Photosynthetic O_2 evolution was measured as a function of dissolved inorganic C and light by means of membrane-inlet mass spectrometry. The diploid stage responded to elevated P_{CO_2} by shunting resources from the production of particulate inorganic C toward organic C yet keeping the production of total particulate C constant. As the effect of ocean acidification was stronger under low light, the diploid stage might be less affected by increased acidity when energy availability is high. The haploid stage maintained elemental composition and production rates under elevated P_{CO_2}. Although both life-cycle stages involve different ways of dealing with elevated P_{CO_2}, the responses were generally modulated by energy availability, being typically most pronounced under low light. Additionally, P_{CO_2} responses resembled those induced by high irradiances, indicating that ocean acidification affects the interplay between energy-generating processes (photosynthetic light reactions) and processes competing for energy (biomass buildup and calcification). A conceptual model is put forward explaining why the magnitude of single responses is determined by energy availability.

The uptake of anthropogenic carbon dioxide (CO_2) by the oceans is causing a significant chemical shift toward higher acidity and P_{CO_2}, a phenomenon known as ocean acidification (OA). As the saturation state for calcium carbonate ($CaCO_3$) concomitantly decreases, calcifying organisms like corals, foraminifers, and coccolithophores have caught the attention of oceanographers, physiologists, and ecologists. Over the past decade, numerous studies have investigated the potential effects of OA on marine calcifiers, especially the coccolithophore *Emiliania huxleyi*. By the formation and export of organic carbon and $CaCO_3$, these bloom-forming unicellular algae sustain vertical gradients of dissolved inorganic C (DIC) and alkalinity (Rost and Riebesell 2004). Furthermore, the $CaCO_3$ can enhance export of aggregated particulate organic matter by ballasting (Klaas and Archer 2002; Lam et al. 2011). As these processes affect the CO_2 exchange with the atmosphere, an influence of OA on these organisms may alter the biogeochemical cycling of C and thereby climate (Zondervan et al. 2001; Rost and Riebesell 2004; Ridgwell et al. 2007).

Riebesell et al. (2000) found that calcification rates decreased with increasing P_{CO_2} in *E. huxleyi* (strain PLYB92/11). Based on these observations, they proposed "reduced marine planktonic calcification" and a rather grim future for calcifiers. Langer et al. (2006), in turn, found nonlinear response patterns or insensitivity in other coccolithophore genera (*Calcidiscus* sp. and *Coccolithus* sp.). Iglesias-Rodriguez et al. (2008) observed increased calcification rates in *E. huxleyi* (strain NZEH) with increasing P_{CO_2}. In a more recent study, Langer et al. (2009) could show that response patterns diverge even between strains, illustrating the difficulties in generalizing OA responses within the *E. huxleyi* morphospecies complex.

Until recently, global change research largely ignored that *E. huxleyi* pursues a haplo-diplontic life cycling, which seems to play a crucial role in its ecology: haploid individuals, for instance, can survive attacks of stage-specific viruses that diminish blooms of diploid individuals. Thus, meiosis is believed to function as an escape strategy (Frada et al. 2008). The haploid stage was found to drive a clearly differentiated metabolism, possibly because of its distinct ecological functionality (Rokitta et al. 2011). It is therefore of interest whether and to which degree the flagellated, noncalcifying life-cycle stage is prone to OA.

Several mechanisms have been put forward in attempt to explain the responses to OA. An increased proton (H^+) concentration may impair transport processes, such as the uptake of inorganic carbon (C_i) or calcium ions (Ca^{2+}), being dependent on electrochemical membrane potentials (Mackinder et al. 2010; Taylor et al. 2011). Increased [CO_2] might directly benefit biomass production either by enhancing the carboxylation reaction at RubisCO (Raven et al. 2005), by reducing CO_2 leakage (Rost et al. 2006), or by allowing a down-regulation of activity of the energy-intensive carbon concentrating mechanism (CCM; Kranz et al. 2010). It has also been indicated that responses to OA are often modulated by light intensities (Kranz et al. 2010; Lefebvre et al. 2010). Investigating the underlying processes as well as the modulating effects of energy availability will therefore improve the understanding of the origins of measured responses.

* Corresponding author: Sebastian.Rokitta@awi.de

In the present study, diploid and haploid cells of *Emiliania huxleyi* (strains 1216 and 1217 from the Roscoff culture collection, RCC) were acclimated to an experimental matrix of present-day vs. elevated P_{CO_2} (38.5 vs. 101.3 Pa) under low vs. high light intensities (50 vs. 300 μmol photons m^{-2} s^{-1}). Besides the assessment of growth rates, cellular quotas of particulate inorganic and organic C (PIC, POC), and particulate organic N (PON), different in vivo assays were conducted to investigate the underlying processes. ^{14}C disequilibrium assays were used to determine the preferential C_i source used for biomass production (CO_2 or HCO_3^-). Photosynthetic O_2 evolution was assessed as a function of [DIC] and light intensities by means of membrane-inlet mass spectrometry (MIMS).

Methods

Culture conditions—Diploid and haploid *Emiliania huxleyi* (strains RCC 1216 and 1217, also known as TQ26 2N and 1N) were obtained from the Roscoff culture collection (www.sb-roscoff.fr/Phyto/RCC). Cells were grown at 15°C in 0.2 μm filtered North Sea seawater (salinity 32), enriched with vitamins and trace metals (Guillard and Ryther 1962). Nitrate and phosphate were added in concentrations of 100 and 6.25 μmol L^{-1}, respectively. Cultures were irradiated with 50 and 300 μmol photons m^{-2} s^{-1} provided by Biolux 965 daylight lamps (Osram) under a 16 : 8-h light : dark (LD) cycle. Light intensities were adjusted using a Li-1400 data logger (Li-Cor) with a 4π sensor (Walz). Cells were preacclimated to the culture conditions for two weeks in medium that was preconditioned by purging with either ambient air (38.5 Pa CO_2) or CO_2-enriched air (101.3 Pa CO_2). CO_2-free air ($<$ 0.1 Pa CO_2; Dominick Hunter) was mixed with pure CO_2 (Air Liquide) by a CGM 2000 mass flow controller system (MCZ Umwelttechnik). The P_{CO_2} was regularly controlled with a nondispersive infrared analyzer system Li-6252 (Li-Cor) that was calibrated with CO_2-free air and purchased air mixtures of 15.2 $\pm$ 0.1 and 101.3 $\pm$ 2.0 Pa CO_2 (Air Liquide). After inoculation, the 900-mL cylindrical flasks were continuously purged with these humidified P_{CO_2}-adjusted gas mixtures to avoid cell sedimentation (flow-rate 130 $\pm$ 10 mL min^{-1}).

Seawater chemistry—To ensure quasi-constant seawater carbonate chemistry (Table 1), only cultures were used for measurements in which the pH did not deviate more than 0.05 units from a cell-free medium (pH measured with pH3000 microprocessor pH-meter; Wissenschaftlich-Technische Werkstätten). The pH electrode was daily calibrated using buffers certified by the U.S. National Bureau of Standards (NBS); obtained values are therefore reported on the NBS scale (pH_{NBS}). DIC was measured colorimetrically according to Stoll et al. (2001), using a TRAACS CS800 autoanalyzer (Seal Analytical). Total alkalinity (TA) was inferred from linear Gran-titration plots (Dickson 1981), which were produced using an automated TitroLine burette system (Schott). Calculations on carbonate chemistry were performed using CO_2SYS (Pierrot et al. 2006) and were based on measurements of pH_{NBS}, TA, temperature, and

Table 1. Carbonate chemistry in the experiment; Attained P_{CO_2}, DIC, HCO_3^-, CO_3^{2-}, and $\Omega_{calcite}$ are calculated based on pH_{NBS} and TA using CO_2Sys (Pierrot et al. 2006). Results are reported for 15°C ($n \geq 3$; $\pm$ SD).

Strain, ploidy	Photon flux (μmol m^{-2} s^{-1})	Treatment P_{CO_2} (Pa)	Attained P_{CO_2} (Pa)	pH_{NBS}	TA (μmol kg^{-1})	DIC (μmol kg^{-1})	HCO_3^- (μmol kg^{-1})	CO_3^{2-} (μmol kg^{-1})	$\Omega_{calcite}$
RCC 1216, 2N	50	Low, 38.5	40.4±0.4	8.112±0.014	2254±20	1997±44	1910±17	140.1±2.1	3.47±0.05
		High, 101.3	97.3±11.1	7.808±0.012	2385±7	2232±22	2186±1	80.0±2.8	1.94±0.07
	300	Low, 38.5	43.5±0.2	8.083±0.040	2273±5	2018±15	1942±4	134.6±0.6	3.33±0.01
		High, 101.3	110.6±14.6	7.741±0.002	2322±35	2174±32	2149±36	68.8±1.9	1.67±0.05
RCC 1217, 1N	50	Low, 38.5	35.6±0.4	8.176±0.005	2393±24	2111±19	1978±21	170.8±2.8	4.23±0.07
		High, 101.3	95.7±1.9	7.823±0.022	2398±3	2249±23	2190±4	83.5±1.5	2.03±0.04
	300	Low, 38.5	35.5±0.4	8.177±0.019	2380±10	2096±24	1967±18	169.5±3.4	4.20±0.08
		High, 101.3	95.2±5.9	7.818±0.038	2402±21	2296±34	2199±14	81.7±7.1	1.98±0.17
Reference	—	Low, 38.5	40.9±1.2	8.134±0.010	2411±13	2134±25	2030±3	156.7±4.9	3.88±0.12
		High, 101.3	100.9±10.4	7.770±0.025	2396±17	2269±45	2171±4	78.2±7.7	1.90±0.19

salinity. For the calculations, phosphate concentrations of 4 μmol L^{-1} were assumed. Dissociation constants of carbonic acid (Mehrbach et al. 1973, refit by Dickson and Millero 1987) and sulfuric acid (Dickson 1990) were used.

Cell growth—In all treatments ($n \geq 3$), cells were harvested in midexponential growth phase 4–6 d after inoculation at densities of 50,000–90,000 cells mL^{-1}. To avoid biases arising from diurnal changes, sampling was done 4–8 h after the beginning of the light period. Cell concentrations were assessed daily using a Multisizer III hemocytometer (Beckman-Coulter), and specific growth rates (μ) were calculated from the daily increments:

$$\mu = (\ln_{c_1} - \ln_{c_0}) \times \Delta t^{-1} \quad (1)$$

where c_0 and c_1 are the initial and final cell concentrations and Δt is the time interval in days.

Elemental composition—For elemental analysis, cells were filtered onto precombusted (12 h, 500°C) GF/F filters (1.2 μm; Whatman) by applying a suction pressure of −20 kPa. To determine cellular POC quotas, respective filters were soaked with 200 μL 0.2 mol L^{-1} HCl (Merck) to remove calcite. Cellular PIC quotas were assessed as the difference in carbon content between the HCl-treated (POC) and untreated filters (total particulate C, TPC). PON measurements were performed on all filters. Analysis was carried out using an automated N and C analyzer SL 20-20 mass spectrometer (SerCon). The multiplication of cellular elemental quotas (POC, PIC, TPC, and PON) with respective specific growth rates yielded daily production rates. Note that these calculated rates are based on estimates of cell density and elemental quotas, which were assessed in a strict time window (Zondervan et al. 2002). Chlorophyll *a* (Chl *a*) quotas were determined fluorometrically after extraction in 90% acetone (Sigma), following the method described by Holm-Hansen and Riemann (1978). The TD-700 fluorometer (Turner Designs) was calibrated with standardized solutions of Chl *a* (Sigma) in 90% acetone.

C_i source—To assess the relative contribution of CO_2 and HCO_3^- to biomass production, the ^{14}C disequilibrium assay (Espie and Colman 1986; Elzenga et al. 2000) was used. Cells were concentrated by gentle filtration (polycarbonate filters, 3 μm; Millipore), and culture medium was successively exchanged with ^{14}C assay medium that was buffered with 50 mmol L^{-1} N,N-Bis(2-hydroxyethyl)glycine (BICINE), having a pH_{NBS} of 8.50 at 15°C. ^{14}C spikes were prepared by adding 10 μL of $NaH^{14}CO_3$ solution (GE Healthcare) to 190 μL deionized water buffered with 20 mmol L^{-1} 4-(2-hydroxyethyl)-1-piperazineethanesulfonic acid (HEPES) having a pH_{NBS} of 7.00 at 20°C, yielding an activity of ~ 740 kBq. Prior to the addition of the ^{14}C spike, 4 mL of stirred cell suspension were irradiated in a temperature-controlled cuvette (15°C) with the respective acclimation light intensity for 6 min to reach steady-state photosynthesis. After the addition of the ^{14}C spike, 200-μL subsamples were taken in short time intervals and dispensed into 2 mL 6 mol L^{-1} HCl to stop vital processes and dissolve calcite. $DI^{14}C$ was removed by degassing. After addition of 10 mL scintillation cocktail (Ultima Gold AB; PerkinElmer), samples were measured with a Tri-Carb liquid scintillation counter (PerkinElmer). Blank measurements were produced using cell-free aliquots of spiked assay medium. Experiments were performed in the presence of 50 μmol L^{-1} dextrane-bound sulfonamide (Ramidus), inhibiting possible external carbonic anhydrase. Time courses of ^{14}C incorporation were used to assess the relative contribution of CO_2 and HCO_3^- to biomass production (Rost et al. 2007).

DIC dependence of photosynthesis—To assess the DIC dependence of photosynthetic O_2 evolution, cells were concentrated by gentle filtration (polycarbonate filters, 3 μm; Millipore), and culture medium was successively exchanged with 50 mmol L^{-1} HEPES-buffered, DIC-free medium (pH_{NBS} 8.20 at 15°C) that was prepared by purging with humidified CO_2-free air for at least 18 h. Eight mL of concentrated cell suspension was transferred to a temperature-controlled cuvette (15°C) that was coupled to a sector-field multicollector mass spectrometer (Isoprime; MicroMass) via a gas-permeable membrane (Polytetrafluorethylen, 0.01 mm) inlet system. In LD intervals with the respective acclimation light intensity, known amounts of DIC were consecutively added in form of $NaHCO_3$ solution during darkness. Net rates of photosynthesis were measured as the change in $[O_2]$ over time. $[O_2]$ signals were two-point calibrated between 0% (after addition of sodium dithionite, an O_2 scavenger) and 21% (as measured in air-equilibrated medium using the solubility coefficient obtained by Weiss 1970). Measured rates of O_2 evolution were corrected for machine-inherent O_2 consumption. The CO_2 baseline was determined by adding NaOH (45 mmol L^{-1} final concentration) into DIC-free assay medium. CO_2 concentrations were calibrated by adding standardized amounts of DIC in form of $NaHCO_3$ solution into 0.2 mol L^{-1} HCl. By adding known amounts of DIC to buffered assay medium, the pH-dependent ratio of $[DIC]:[CO_2]$ was determined. By the addition of carbonic anhydrase (1 μg; Sigma) to the assay, rapid equilibration of the carbonate system was assured, allowing the calculation of [DIC] from the recorded CO_2 signals. Obtained kinetic curves were fit with the Michaelis–Menten equation:

$$P = \frac{V_{max} \times [S]}{K_{1/2} + [S]} \quad (2)$$

where P is the net rate of photosynthesis, V_{max} is the DIC-saturated net rate of photosynthesis, [S] is the substrate concentration (i.e., [DIC]), and $K_{½}$ is the half-saturation concentration for the substrate.

Light dependence of photosynthesis—To assess the light dependence of photosynthetic O_2 evolution, cells were concentrated as described above and medium was exchanged with air-equilibrated 50 mmol L^{-1} HEPES-buffered assay

medium (pH_{NBS} 8.20 at 15°C). Net rates of photosynthesis were measured as described above. Photosynthesis vs. irradiance curves were fit using the following equation:

$$P = V_{max} \times \left(1 - e^{(-b \times (I-c))}\right) \quad (3)$$

where P is the net photosynthetic rate, V_{max} is the light-saturated net rate of photosynthesis, and I is the irradiance. The light intensity at which the photosynthesis starts to enter saturation (i.e., light acclimation index, I_k) and the initial light-limited slope of the curve (i.e., maximum light-use efficiency, α) were calculated according to the following:

$$I_k = b^{-1} + c \quad (4)$$

$$\alpha = V_{max} \times b \quad (5)$$

Statistics—For parameters that were calculated by multiplication from error-afflicted values (i.e., production rates, Chl *a* : POC), error propagation was taken into account: relative propagated standard deviations ($SD_{rel;prop}$) were calculated as the square root of the sum of the squared relative standard deviations ($SD_{rel;1,2}$):

$$SD_{rel;prop} = \sqrt[2]{\left(SD_{rel;1}{}^2\right) + \left(SD_{rel;2}{}^2\right)} \quad (6)$$

Statistical significances of data were obtained by applying two-way ANOVAs to the full data matrix of P_{CO_2} vs. light vs. ploidy. The null hypothesis was withdrawn when the ANOVA *p*-values were < 0.05. To obtain significances between means, Tukey's honestly significant difference statistic was applied for post hoc testing. If not stated otherwise, results were called significant at a 95% confidence level, that is, when *p*-values were ≤ 0.05. In all measurements, the sample size of biological replicates *n* was ≥ 3.

Results

Because of the chosen matrix approach, results of the treatments can be viewed from two directions: the effects of P_{CO_2} can be modulated as a result of altered light intensity, and, vice versa, light-induced effects can be modulated by P_{CO_2}. To maintain scope and clarity of this study, the following sections exclusively focus on CO_2 effects and their modulation by light. Results are presented separately for each particular life-cycle stage.

The diploid life-cycle stage—Growth rates of the diplont were not significantly affected by elevated P_{CO_2} under both light conditions (Fig. 1a). In response to elevated P_{CO_2}, the POC quota increased significantly under high (+59%) and low light conditions (+40%; Table 2). The production rates of POC in the diploid cells reacted to elevated P_{CO_2} with a prominent increase under low light (+84%), whereas this effect was attenuated under high light (Fig. 1b). The PIC quota significantly decreased with elevated P_{CO_2} under low light (−77%) but not under high light (Table 2). Consequently, PIC production was strongly reduced under low light (−74%) but not under high light (Fig. 1c). The PIC : POC ratio of the diploid cells decreased under elevated P_{CO_2} (Table 2). This effect is highly significant under low light (−85%) but attenuated under high light conditions. Regarding the production of TPC, however, no alterations were observed in response to elevated P_{CO_2} (Fig. 1d). Under elevated P_{CO_2}, PON quotas of the diploid stage increased significantly under low (+84%) and high light conditions (+51%; $p = 0.051$, significant at a 90% confidence level; Table 2). As these quotas closely followed the trends of the respective POC quotas, no effects of P_{CO_2} on the POC : PON ratio (Table 2) were observed. Cellular Chl *a* quotas were not affected by P_{CO_2} (Fig. 1e). When normalized to POC, however, Chl *a* contents (Chl *a* : POC) decreased notably in response to elevated P_{CO_2} under low light (−29%), whereas this decrease was less pronounced under high light (Fig. 1f).

Regarding the source of inorganic carbon, ^{14}C disequilibrium assays revealed that in the diploid stage, HCO_3^- contribution (75–90%) was not altered by P_{CO_2} under low light but decreased slightly under high light (−11%; Fig. 2a). MIMS-based affinity assays could not show any alterations of half-saturation concentrations for DIC ($K_{½}$;DIC) in response to elevated P_{CO_2} (Fig. 2b). Regarding the light dependence of O_2 evolution, Chl *a*-normalized maximum photosynthetic rates ($V_{max;Chl}$) decreased in response to elevated P_{CO_2}, an effect that was significant under low light (−45%) but not under high light (Fig. 2c). Cell-normalized maximum rates ($V_{max;cell}$) under elevated P_{CO_2} decreased significantly under low light (−59%) but not under high light (Fig. 2d). The I_k values and Chl *a*-normalized maximum light-use efficiencies (α_{Chl}) of the diploid stage were not affected by P_{CO_2} (Table 2). Cell-normalized maximum light-use efficiencies (α_{cell}), however, decreased significantly under low light (−40%), whereas this effect was insignificant under high light (Table 2). Under in situ light intensities, cell-normalized net rates of photosynthesis of the diploid stage ($V_{in\ situ;cell}$) significantly decreased in response to elevated P_{CO_2} under low light (−48%), but not under high light (Fig. 2f). After normalization to Chl *a*, however, $V_{in\ situ;Chl}$ is not affected by P_{CO_2} in any of the light treatments (Fig. 2e).

The haploid life-cycle stage—In the haplont, elevated P_{CO_2} leads to significant decreases in growth rates under both low light (−14%; $p = 0.06$, i.e., significant at a 90% confidence level) and high light (−28%; Fig. 1a). Quotas of POC were not significantly affected by elevated P_{CO_2} under both light conditions (Table 2). Likewise, POC productions were not significantly altered by P_{CO_2} (Fig. 1b). PIC quotas measured in the haploid stage were < 1 pg cell^{-1} in all treatments, reflecting the absence of calcification (Fig. 1c). Also, the PON quotas were not significantly altered by elevated P_{CO_2} (Table 2). Consequently, POC : PON ratios were unaffected by elevated P_{CO_2} (Table 2). Chl *a* quotas of the haplont decreased significantly in response to elevated P_{CO_2} under low light (−31%), whereas the effect was attenuated under high light (Fig. 1e). Chl *a* : POC decreased prominently in response to elevated P_{CO_2} under low light (−47%) but not under high light (Fig. 1f).

Regarding C_i acquisition, the contribution of HCO_3^- to C fixation (83–90%) was not influenced by P_{CO_2} (Fig. 2a).

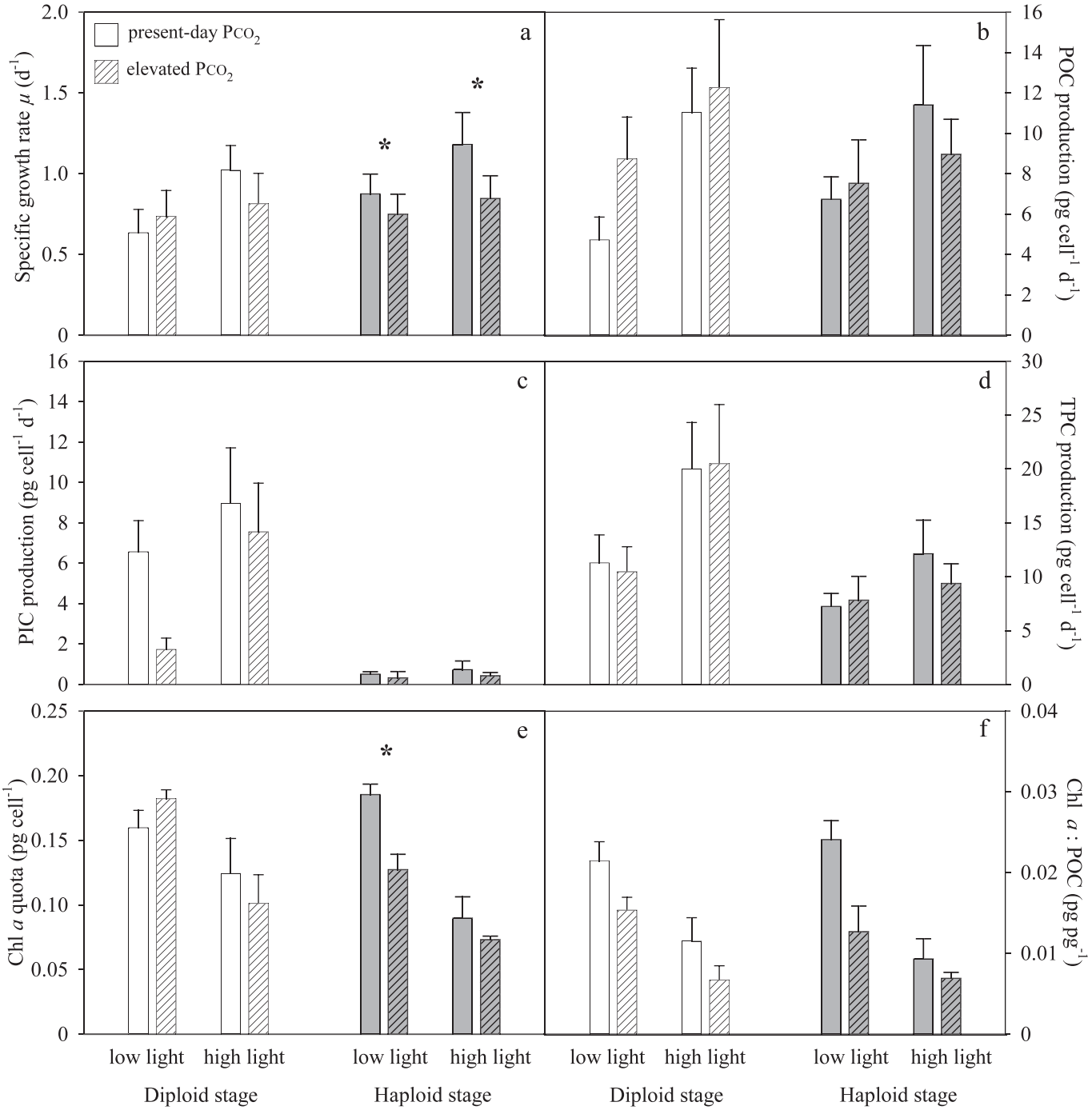

Fig. 1. Phenomenological responses of diploid (white) and haploid (gray) *Emiliania huxleyi* (RCC1216 and 1217) to present-day P_{CO_2} (filled; 38.5 Pa) and elevated P_{CO_2} (shaded, 101 Pa) under low (50 μmol photons m^{-2} s^{-1}) and high (300 μmol photons m^{-2} s^{-1}) light intensity. Error bars denote 1 SD ($n \geq 3$).

Yet, in response to elevated P_{CO_2}, $K_{1/2}$ (DIC) increased significantly under low light (+409%), an effect that was attenuated under high light (Fig. 2b). No significant effects on $V_{max;Chl}$ were observed in response to P_{CO_2} under both light conditions (Fig. 2c). Values of $V_{max;cell}$, however, decreased significantly in response to elevated P_{CO_2} under both, low (−52%) and high light conditions (−40%; Fig. 2d). I_k values decreased significantly as an effect of elevated P_{CO_2} under low (−51%; $p = 0.06$, i.e., significant at a 90% confidence level) and high light conditions (−58%; Table 2). Elevated P_{CO_2} caused significant increases in α_{Chl} under low light (+84%) and high light (+187%; Table 2) conditions. Cell-normalized light-use efficiencies (α_{cell}) were, however, insensitive to P_{CO_2} (Table 2). Values of $V_{in\ situ;Chl}$ increased significantly in response to elevated P_{CO_2} under high (+74%; $p = 0.06$, i.e., significant at a 90% confidence level) but not under low light (Fig. 2e). Values of $V_{in\ situ;cell}$ were, however, not affected by P_{CO_2} (Fig. 2f).

Table 2. Responses of diploid and haploid *Emiliania huxleyi* (RCC 1216 and 1217; 2N and 1N) grown under low P_{CO_2} (38.5 Pa) and elevated P_{CO_2} (101.3 Pa) under low (50 μmol photons m^{-2} s^{-1}) and high (300 μmol photons m^{-2} s^{-1}) light intensity. Errors denote 1 SD ($n \geq 3$). Light intensity (μmol photons m^{-2} s^{-1}); specific growth rate (d^{-1}); quotas (pg $cell^{-1}$); productions (pg $cell^{-1}$ d^{-1}); PIC : POC, POC : PON, HCO_3^- uptake : net fixation (mol mol^{-1}); Chl *a* : POC (pg pg^{-1}); $K_{½}$ (DIC) (μmol kg^{-1}); $V_{max;Chl}$, $V_{in\ situ;Chl}$ (μmol O_2 [mg Chl *a*]$^{-1}$ h^{-1}); $V_{max;cell}$, $V_{in\ situ;cell}$ (fmol O_2 $cell^{-1}$ h^{-1}); I_k (μmol photons m^{-2} s^{-1}); α_{Chl} (μmol O_2 [mg Chl *a*]$^{-1}$ h^{-1} [μmol photons m^{-2} s^{-1}]$^{-1}$); α_{cell} (fmol O_2 $cell^{-1}$ h^{-1} [μmol photons m^{-2} s^{-1}]$^{-1}$).

Strain, ploidy	RCC 1216, 2N				RCC 1217, 1N			
Light intensity	50		300		50		300	
P_{CO_2} treatment	38.5	101.3	38.5	101.3	38.5	101.3	38.5	101.3
Specific growth rate	0.63±0.14	0.74±0.16	1.02±0.15	0.81±0.19	0.87±0.12	0.75±0.12	1.18±0.20	0.85±0.14
POC quota	7.45±0.54	11.87±1.14	10.81±1.41	15.08±2.20	7.70±0.67	10.04±2.34	9.65±1.90	10.58±1.05
PIC quota	10.35±0.63	2.35±0.58	8.78±2.34	9.29±2.03	0.58±0.12	0.43±0.41	0.61±0.35	0.51±0.16
PON quota	1.25±0.08	2.31±0.29	1.52±0.37	2.29±0.39	1.49±0.15	2.07±0.56	1.63±0.35	1.93±0.20
PIC : POC	1.40±0.16	0.20±0.07	0.82±0.22	0.65±0.19	0.07±0.01	0.06±0.03	0.06±0.04	0.05±0.02
POC : PON	6.97±0.31	5.95±0.91	7.48±0.26	7.75±0.63	6.00±0.13	5.84±0.56	6.92±0.33	6.71±0.30
POC production	4.72±1.13	8.73±2.07	11.03±2.19	12.27±3.36	6.73±1.11	7.52±2.15	11.40±2.94	8.96±1.74
PIC production	6.56±1.55	1.73±0.57	8.96±2.74	7.55±2.41	0.51±0.12	0.32±0.31	0.73±0.43	0.43±0.15
TPC production	11.29±2.59	10.46±2.31	20.00±4.32	20.49±5.49	7.24±1.21	7.81±2.21	12.12±3.11	9.37±1.83
PON production	0.79±0.19	1.70±0.42	1.55±0.44	1.87±0.54	1.30±0.23	1.55±0.49	1.93±0.53	1.63±0.32
Chl *a* quota	0.16±0.01	0.18±0.01	0.12±0.03	0.10±0.02	0.19±0.01	0.13±0.01	0.09±0.02	0.07±0.00
Chl *a* : POC	0.02±0.00	0.02±0.00	0.01±0.00	0.01±0.00	0.02±0.00	0.01±0.00	0.01±0.00	0.01±0.00
HCO_3^- uptake : net fixation	0.85±0.01	0.86±0.04	0.89±0.03	0.76±0.05	0.87±0.01	0.87±0.03	0.89±0.03	0.83±0.05
$K_{½}$ (DIC)	111±110	114±62	20±20	50±43	66±48	333±72	126±81	156±135
$V_{max;Chl}$	451±33	246±16	505±81	378±69	300±50	270±59	254±38	307±66
$V_{max;cell}$	49±3	20±5	36±4	26±6	39±7	19±5	21±4	13±2
$V_{in\ situ;Chl}$	116±17	81±25	445±55	348±57	66±31	113±21	167±48	290±64
$V_{in\ situ;cell}$	13±2	7±2	32±2	24±5	8±4	8±1	14±4	12±2
I_k	121±6	91±16	151±21	124±13	160±45	79±24	293±65	123±9
α_{Chl}	4.47±0.52	3.66±0.71	3.94±0.23	3.32±0.37	2.29±0.91	4.21±0.61	1.15±0.38	3.30±0.71
α_{cell}	0.49±0.05	0.29±0.04	0.29±0.02	0.23±0.04	0.29±0.11	0.29±0.03	0.10±0.04	0.14±0.03

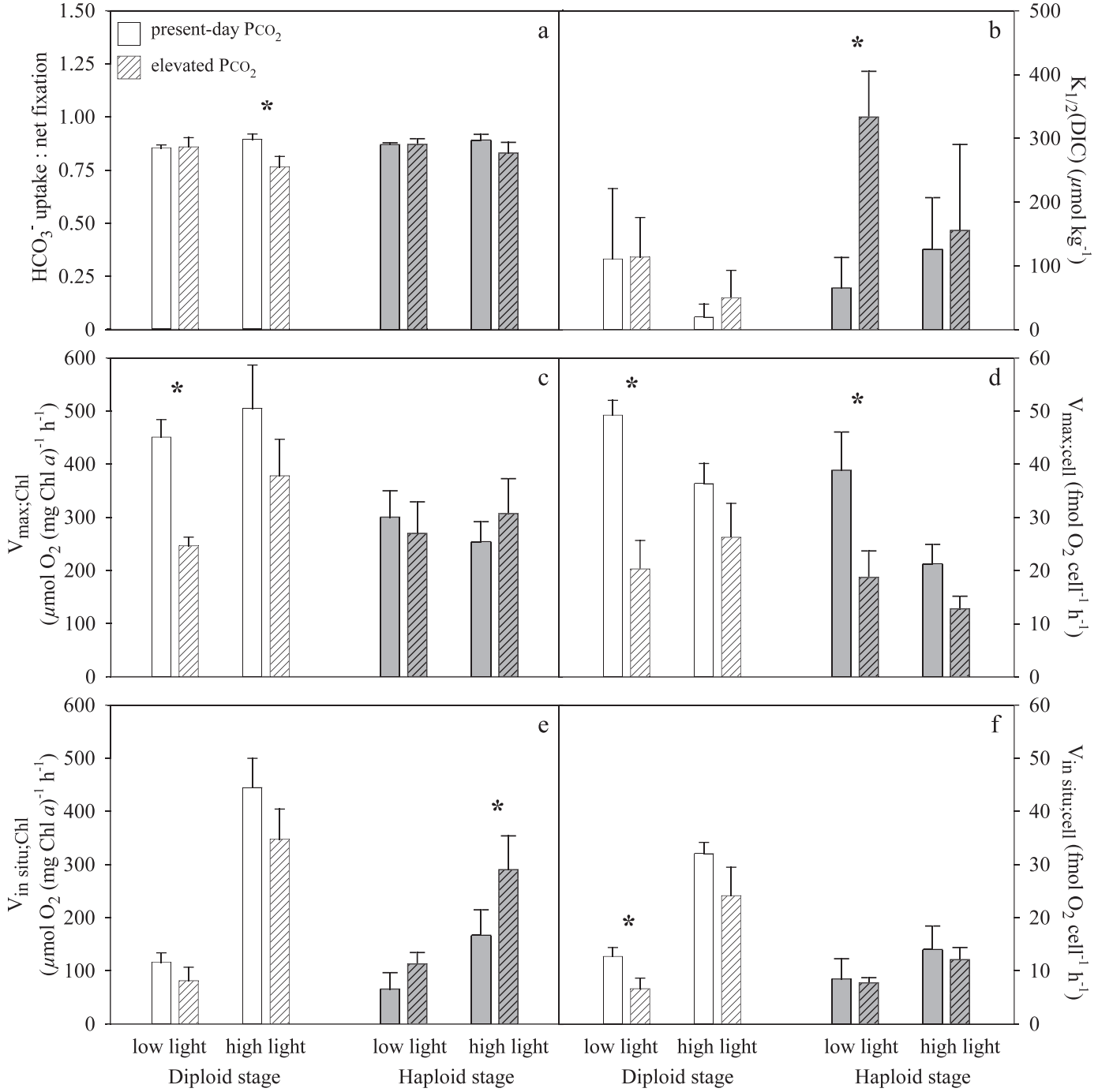

Fig. 2. Physiological responses of diploid (white) and haploid (gray) *Emiliania huxleyi* (RCC1216 and 1217) to present-day P_{CO_2} (filled; 38.5 Pa) and elevated P_{CO_2} (shaded, 101 Pa) under low (50 μmol photons m^{-2} s^{-1}) and high (300 μmol photons m^{-2} s^{-1}) light intensity. Error bars denote 1 SD (n = 3).

Discussion

The life-cycle stages of *E. huxleyi* represent independent entities with strikingly divergent features (Frada et al. 2008; Von Dassow et al. 2009; Rokitta et al. 2011). A direct comparison of measured parameters between them is therefore obsolete. For this reason, the effects of P_{CO_2} and their modulation by light are first evaluated separately for the diplont and haplont and, at a later stage, discussed synoptically.

The diploid life-cycle stage—Cellular quotas and production rates of POC and PIC were affected by P_{CO_2} (Fig. 1b,c; Table 2). Elevated P_{CO_2} stimulated POC production, while production rates of PIC were reduced (Fig. 1b,c). Similar response patterns were observed in the

strain PLYB92/11 (Riebesell et al. 2000; Zondervan et al. 2002): Under 150 μmol photons m^{-2} s^{-1}, for instance, POC production increased from 9.0 to 9.8 pg $cell^{-1}$ d^{-1}, while PIC production decreased from 9.2 to 7.6 pg $cell^{-1}$ d^{-1} over a P_{CO_2} range of about 15.2 to 81.1 Pa. The findings of the present study are also in line with Langer et al. (2009), who found comparable responses in strain RCC1216 grown under 400 μmol photons m^{-2} s^{-1}. Richier et al. (2011) found small yet insignificant increases in POC and PIC production under OA in this same strain, which may originate from different culture conditions (e.g., smaller P_{CO_2} range of 44.6 vs. 78.0 Pa). Although the comparable studies differ in terms of absolute values and trends, POC and PIC production typically exhibited opposing trends. This anticorrelation, reflected by decreasing PIC : POC ratios in response to elevated P_{CO_2} is widely observed in strains of the *E. huxleyi* morphospecies complex (Riebesell et al. 2000; Langer et al. 2009; Feng et al. 2008) and has often been used to demonstrate the exceptionally high sensitivity of coccolithophores to OA.

TPC production was not affected by P_{CO_2} (Fig. 1d). Although not explicitly stated, quasi-constant TPC productions were reported in a number of other studies. In Zondervan et al. (2002), TPC productions (as calculated from averaged growth rates and PIC and POC quotas) were independent of P_{CO_2} over a range 15.2 to 81.1 Pa (20.7 $\pm$ 1.3 and 18.3 $\pm$ 0.9 pg TPC $cell^{-1}$ under light intensities of 80 and 150 μmol photons m^{-2} s^{-1}, respectively). Likewise, Langer et al. (2009) found unaltered rates of TPC production in strain RCC1216 (24.0 $\pm$ 1.6 pg TPC $cell^{-1}$) over a P_{CO_2} range of 22.3 to 121.6 Pa. In the study of Feng et al. (2008), clear effects of P_{CO_2} on TPC productions are also lacking in most treatments. Only at high temperature (24°C), a slight P_{CO_2}-related effect can be recognized. The apparent insensitivity in TPC production toward changes in P_{CO_2} suggests that the overall acquisition of inorganic carbon is not generally hampered yet that carbon is differently allocated among cellular processes under OA.

To explore the origins of these phenomena, in vivo assays were conducted to assess properties of carbon acquisition. ^{14}C disequilibrium assays demonstrated that HCO_3^- is the major source of inorganic carbon for photosynthetic C fixation in all P_{CO_2} treatments (75–90%; Fig. 2a). This corresponds to earlier studies on *E. huxleyi*, showing that diploid cells operate a CCM based mainly on HCO_3^- uptake (Trimborn et al. 2007), for which now also preliminary molecular evidence exists (Von Dassow et al. 2009; Rokitta et al. 2011). Regarding the affinities for inorganic carbon, $K_{½}$ (DIC) values were low and not significantly altered in response to P_{CO_2} (Fig. 2b), indicating C_i saturation of transporters under in situ conditions. Affinities were similar to previously obtained values for diploid cells grown under comparable conditions (36.5 Pa CO_2; 180 μmol photons m^{-2} s^{-1}; 16 : 8-h LD cycle; Rost et al. 2006). The slightly lower $K_{½}$ (DIC) values under high light may be attributed to a higher energization of the C_i uptake system (Beardall 1991) or a generally higher C_i demand (Rost et al. 2006), as also indicated by higher TPC productions (Fig. 1d).

Parameters of light-dependent photosynthesis, that is, maximum as well as in situ rates of O_2 evolution (Fig. 2c–f) and maximum light-use efficiencies (Table 2), decreased in response to elevated P_{CO_2}. Such responses are typically observed in the context of light acclimations, indicating decreased energy generation under high light (MacIntyre et al. 2002). A large part of this photoacclimation usually originates from a lowered Chl *a* : POC ratio, which is also the case under elevated P_{CO_2} (Fig. 1f). The observed similarities between effects of high light and elevated P_{CO_2} indicate that the throttling of energy generation is a common mechanism not only to cope with a high energy supply but also to adjust to a decreased energy demand. Feng et al. (2008) observed an apparently opposing trend, that is, an increase in photosynthesis under elevated P_{CO_2}. However, while Feng and coworkers assessed net ^{14}C incorporation into biomass over 24 h, in this study net rates of O_2 evolution were measured over several minutes during midday. Note that comparability between methods is given only when measurements use similar units and time frames. When considering the more comparable data on biomass production, that is, the increased buildup of POC under elevated P_{CO_2} (Fig. 1b), both studies in fact show consistent trends.

To sum up, the diploid cells maintain their TPC production rates under elevated P_{CO_2} by reallocating acquired resources from PIC toward POC production (Fig. 1b–d). As C_i acquisition appears unaltered in the assays, the shunting of resources likely originates from processes that occur downstream of the C_i accumulation. Also, these processes might be responsive to $[H^+]$ rather than C_i concentrations (Taylor et al. 2010; Lefebvre et al. 2012). Suffrian et al. (2011) have shown that external pH perturbations translate linearly into cytoplasmic pH changes. An impairment of transport processes (e.g., for DIC and Ca^{2+}) due to low internal pH might weaken the process of biomineralization. In any case, the anticorrelation between PIC and POC production once more stresses that calcification is neither a prerequisite nor a means for supporting C fixation (Trimborn et al. 2007).

Despite lowered photosynthetic energy generation under elevated P_{CO_2} (Fig. 2e,f), the diploid cells maintain and even increase production rates of TPC and POC, respectively (Fig. 1b,d). One reason for these P_{CO_2}-dependent changes in energy efficiency might be a downregulation of CCM activity. For example, decreased leakage of actively accumulated CO_2 may supersede part of the CCM activity under elevated P_{CO_2}. A down-regulation might therefore liberate significant amounts of energy (Kranz et al. 2010). Although assay results that are obtained under constant pH do not indicate significant alterations in C_i source and affinities (Fig. 2a,b), the CCM activity may in fact be altered under in situ carbonate chemistry. Especially in the ^{14}C-disequilibrium assay, the high pH of 8.5 deviates strongly from in situ pH values being lower than 7.9 in the high P_{CO_2} treatments (Table 1). Consequently, the assay results might be biased because C_i transporters are reacting not only to CO_2 and HCO_3^- availability but also to $[H^+]$. In view of these shortcomings, assay conditions should be modified to resemble in situ pH values.

Light strongly modulated the magnitude of the P_{CO_2} responses (Figs. 1, 2). Under energetic constraints, that is, low light, the effect of elevated P_{CO_2} was typically most pronounced. As discussed above, an altered energetic status of the cells may originate from down-regulation of CCM activity. The impairment of calcification under elevated P_{CO_2} may reduce the ability of this process to compete with POC production for resources like C_i and energy. This detrimental effect of OA can apparently be compensated by higher energy supply; that is, PIC production is partially reestablished when light intensity is high (Fig. 1c).

The haploid life-cycle stage—Neither the quotas of POC and PON nor the respective production rates were significantly altered by elevated P_{CO_2} (Table 2; Fig. 1b), suggesting that overall productivity of haploid *E. huxleyi* cells is only marginally affected by OA. Also, the POC : PON ratios were independent from P_{CO_2} but increased slightly with light (Table 2), emphasizing that the processes of carbon fixation and nitrogen acquisition are tightly coupled (under N-replete conditions) and depend on energy availability rather than carbonate chemistry. In vivo assays resolved that the described maintenance of elemental composition and the absence of clear macroscopic effects can be attributed to adjustments within C_i acquisition and photophysiology.

^{14}C disequilibrium assays could show that HCO_3^- is the major C_i source ($\sim$ 80–90%) and that the fractional contribution to biomass buildup is not altered by elevated P_{CO_2} (Fig. 2a). MIMS-based assays could resolve that elevated P_{CO_2} leads to decreased C_i uptake affinities under low light but not under high light (Fig. 2b). Decreased C_i affinities in response to elevated P_{CO_2} have been reported for diploid *E. huxleyi* (strain PLYB92/11; Rost et al. 2003), a number of diatoms (Trimborn et al. 2008), and also cyanobacteria (Sültemeyer et al. 1998). The latter study suggests posttranslational modification being responsible for decreased affinities under elevated P_{CO_2}.

Regarding the light dependence of O_2 evolution, the Chl *a*–normalized maximum net rates of photosynthesis ($V_{max;Chl}$) are not affected by elevated P_{CO_2} (Fig. 2c), indicating that the photosystems can in principle deliver the same energetic output when light saturated. Photosystems do, however, not perform equally well at acclimation light intensities, which is indicated by higher Chl *a*–normalized in situ rates under elevated P_{CO_2} ($V_{in\ situ;Chl}$; Fig. 2e). As cellular Chl *a* quotas are, however, themselves affected by the treatments, cell normalization yields more meaningful measures: accounting for this, cellular in situ rates of photosynthesis were not affected by elevated P_{CO_2} ($V_{in\ situ;cell}$; Fig. 2f); that is, cells generate the same amount of photosynthetic energy. The down-regulation in Chl *a* content and $V_{max;cell}$ under elevated P_{CO_2} resembles responses typically observed in high light acclimations (McIntyre et al. 2002).

To sum up, haploid cells adjust their metabolism to elevated P_{CO_2}, resulting in constant productivity, elemental composition, and cellular energy budget. The unaltered cellular in situ rates of photosynthesis despite lowered Chl *a* : POC indicate improved energy efficiency under elevated P_{CO_2}. As suggested for the diploid stage, improved CO_2 supply might in part supersede CCM activity and reduce the costs associated with active C_i acquisition. The fact that the haploid cells down-scale light harvesting instead of enhancing biomass production under elevated P_{CO_2} is in line with the parsimonious lifestyle that was proposed from transcriptomic analyses (Von Dassow et al. 2009; Rokitta et al. 2011).

Synopsis and conceptual model—A common trait of both life-cycle stages is the quasi-constant TPC production under elevated P_{CO_2}, which is also in line with the P_{CO_2} insensitivity in POC : PON ratios observed (Table 2). This unaltered "productivity" might originate from cell-physiological constraints, such as surface : volume ratio, transporter density, or macromolecular composition. Regarding the P_{CO_2} effects on pigment contents, the haplont keeps its POC quotas constant but decreases its Chl *a* quota, whereas the diploid stage increases POC quotas and maintains its Chl *a* quota. The result in both stages, however, is a reduction of Chl *a* : POC, indicating decreased light harvesting under elevated P_{CO_2}.

Despite this down-regulation in light harvesting, cells of both stages were able to maintain or increase TPC or POC productions, suggesting improved energy efficiency under elevated P_{CO_2}. Furthermore, observed CO_2 responses were typically pronounced under low light and minimized under high light. This can be explained when considering applied conditions, such as elevated P_{CO_2}, as energetically beneficial or adverse for any defined metabolic process that follows a typical saturation kinetic (Fig. 3). While the energetic status of the cell is governed primarily by light, secondary treatments may further increase or decrease the amount of energy that is available to the process. The saturation behavior explains why the same absolute energetic benefit or detriment (here induced by elevated P_{CO_2}) causes responses of different magnitudes, depending on the light levels. In the case of POC production, elevated P_{CO_2} increases the available energy and thereby stimulates biomass production in the diplont. In the case of PIC production, elevated P_{CO_2} apparently increases the costs, thereby lowering available energy and reducing calcification. In other words, the overall energetic status of the cell (governed by environmental parameters, primarily light) determines whether responses to energetically relevant environmental changes are large or small. This conceptual model might explain some of the apparent variability in OA responses observed within the *E. huxleyi* morphospecies complex (Langer et al. 2009; Hoppe et al. 2011) and even within a single strain (Langer et al. 2009; Richier et al. 2011; this study).

This interdependence of responses toward changing environmental conditions emphasizes the multidimensionality of physiological processes. Studies have shown that changes in energetically relevant environmental parameters, especially P_{CO_2} and light, are mutually influencing (Smith 1936; this study). In addition to the assessment of modulated effects, the application of such multifactorial matrices and the ceteris paribus principle further allows the identification of causal relationships. Clearly, these

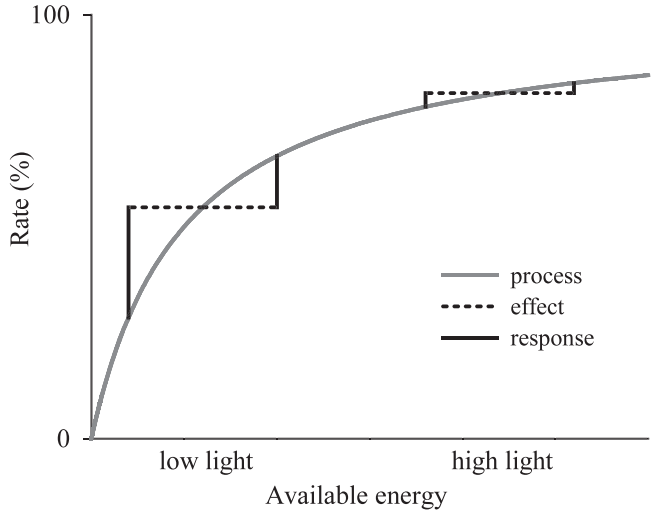

Fig. 3. Energy-dependent modulation of physiological responses to an environmental parameter. The rate of a physiological process (gray line) is governed primarily by energy supply (i.e., irradiance). Changes in other environmental parameters (e.g., P_{CO_2}) cause additional, adverse or beneficial effects (dotted black lines) on the overall energy availability. Although these effects are of the same magnitude, the responses (solid black lines), that is, the changes in process rates, are notably stronger under low energy availability.

approaches deepen the understanding of cellular mechanisms that underlie the observed phenomena. It is therefore to be appreciated that experiments are increasingly conducted using different combinations of relevant environmental conditions (Feng et al. 2008; Kranz et al. 2010; Shi et al. 2010).

Ecological and biogeochemical implications—Our findings show that the responses to OA are strongly modulated by light. In the natural environment, the vertical motion of water masses causes the phytoplankton to experience a broad range of light intensities. As OA effects were diminished at higher light intensities, that is, at the surface ocean, the rise in P_{CO_2} will mostly affect specimens residing at lower irradiances, that is, at the lower photic zone. Blooms of *E. huxleyi*, however, tend to develop under highly stratified conditions (Tyrrell and Merico 2004), and thus the concomitant high mean irradiances may partially attenuate OA effects. Even though OA effects on physiology appear small at times, such as under high light, they may translate into large ecological consequences in the real world, where competition and grazing play a crucial role. Floristic shifts due to OA have been observed within the group of coccolithophores, lightly calcified strains being favored over heavily calcified ones (Beaufort et al. 2011). Investigations on combined effects of abiotic and biotic factors, conducted in monoclonal as well as in field populations, are needed to understand and predict the fate of coccolithophore calcification in the framework of global change.

In terms of consequences for elemental cycling, the effects of OA on the haploid life-cycle stage are not likely to translate into biogeochemically significant effects. In the diploid stage, which probably constitutes the primal part of the life cycle, the alterations in PIC and POC productions may have implications for the depth export not only of alkalinity but also of organic material. The likely lowered vertical flux of alkalinity in the future may increase the uptake capacity of surface waters for anthropogenic CO_2 (Zondervan et al. 2001). A lowered degree of calcification could, however, also hamper the vertical export of organic carbon due to lowered ballasting (Klaas and Archer 2002), in turn leading to decreased C drawdown from surface waters (Lam et al. 2011). Further assessment of the relative strengths of the biological carbon pumps and their interdependence is needed for thorough predictions of carbon cycling in contemporary and future oceans.

Acknowledgments

We gratefully acknowledge the assistance of Klaus-Uwe Richter and Ulrike Richter, who administrated the mass spectrometers used for data acquisition. We further thank Uwe John and Dieter Wolf-Gladrow for constructive comments on the manuscript. This work was funded by the European Research Council (ERC) under the European Community's Seventh Framework Programme (FP7/2007-2013), ERC grant agreement 205150, and contributes to the European Project on Ocean Acidification (EPOCA), grant agreement 211384.

References

Beardall, J. 1991. Effects of photon flux density on the "CO_2 concentrating mechanism" of the cyanobacterium *Anabaena variabilis*. J. Plankton Res. **13:** 133–141.

Beaufort, L., and others. 2011. Sensitivity of coccolithophores to carbonate chemistry and ocean acidification. Nature **476:** 80–83, doi:10.1038/nature10295

Dickson, A. G. 1981. An exact definition of total alkalinity and a procedure for the estimation of alkalinity and total inorganic carbon from titration data. Deep-Sea Res. **28:** 609–623, doi:10.1016/0198-0149(81)90121-7

———. 1990. Standard potential of the reaction: AgCl(s) + ½ H_2(g) = Ag(s) + HCl(aq), and the standard acidity constant of the ion HSO_4^- in synthetic seawater from 273.15 to 318.15 K. J. Chem. Thermodyn. **22:** 113–127, doi:10.1016/0021-9614(90)90074-Z

———, and F. J. Millero. 1987. A comparison of the equilibrium constants for the dissociation of carbonic acid in seawater media. Deep-Sea Res. **34:** 1733–1743, doi:10.1016/0198-0149(87)90021-5

Elzenga, J. T. M., H. B. A. Prins, and J. Stefels. 2000. The role of extracellular carbonic anhydrase activity in inorganic carbon utilization of *Phaeocystis globosa* (Prymnesiophyceae): A comparison with other marine algae using the isotopic disequilibrium technique. Limnol. Oceanogr. **45:** 372, doi:10.4319/lo.2000.45.2.0372

Espie, G. S., and B. Colman. 1986. Inorganic carbon uptake during photosynthesis—a theoretical analysis using the isotopic disequilibrium technique. Plant Physiol. **80:** 863–869, doi:10.1104/pp.80.4.863

Feng, Y., M. E. Warner, Y. Zhang, J. Sun, F. X. Fu, J. M. Rose, and D. A. Hutchins. 2008. Interactive effects of increased P_{CO_2}, temperature and irradiance on the marine coccolithophore *Emiliania huxleyi* (Prymnesiophyceae). Eur. J. Phycol. **43:** 78–98, doi:10.1080/09670260701664674

Frada, M., I. Probert, M. J. Allen, W. H. Wilson, and C. De Vargas. 2008. The "Cheshire Cat" escape strategy of the coccolithophore *Emiliania huxleyi* in response to viral infection. PNAS **105:** 15944–15949, doi:10.1073/pnas.0807707105

Guillard, R. R. L., and J. H. Ryther. 1962. Studies of marine planktonic diatoms. Can. J. Microbiol. **8:** 229–239, doi:10.1139/m62-029

Holm-Hansen, O., and B. Riemann. 1978. Chlorophyll *a* determination: Improvements in methodology. Oikos **30:** 438–447, doi:10.2307/3543338

Hoppe, C. J. M., G. Langer, and B. Rost. 2011. *Emiliania huxleyi* shows identical responses to elevated P_{CO_2} in TA and DIC manipulations. JEMBE **406:** 54–62, doi:10.1016/j.jembe.2011.06.008

Iglesias-Rodriguez, M. D., and others. 2008. Phytoplankton calcification in a high-CO_2 world. Science **320:** 336–340, doi:10.1126/science.1154122

Klaas, C., and D. E. Archer. 2002. Association of sinking organic matter with various types of mineral ballast in the deep sea: Implications for the rain ratio. Glob. Biogeochem. Cycles **16:** 1116, doi:10.1029/2001GB001765

Kranz, S. A., O. Levitan, K.-U. Richter, O. Prasil, I. Berman-Frank, and B. Rost. 2010. Combined effects of CO_2 and light on the N_2-fixing cyanobacterium *Trichodesmium* IMS101: Physiological responses. Plant Physiol. **154:** 334–345, doi:10.1104/pp.110.159145

Lam, P. J., S. C. Doney, and J. K. B. Bishop. 2011. The dynamic ocean biological pump: Insights from a global compilation of particulate organic carbon, $CaCO_3$, and opal concentration profiles from the mesopelagic. Glob. Biogeochem. Cycles **25:** 1–14, doi:10.1029/2010GB003868

Langer, G., M. Geisen, K. H. Baumann, J. Kläs, U. Riebesell, S. Thoms, and J. R. Young. 2006. Species-specific responses of calcifying algae to changing seawater carbonate chemistry. Geochem. Geophys. Geosyst. **7:** 1–12, doi:10.1029/2005GC001227

———, G. Nehrke, I. Probert, J. Ly, and P. Ziveri. 2009. Strain-specific responses of *Emiliania huxleyi* to changing seawater carbonate chemistry. Biogeosciences **6:** 2637–2646, doi:10.5194/bg-6-2637-2009

Lefebvre, S. C., G. Harris, R. Webster, N. Leonardos, R. J. Geider, and C. A. Raines. 2010. Characterization and expression analysis of the *Lhcf* gene family in *Emiliania huxleyi* (Haptophyta) reveals differential responses to light and CO_2. J. Phycol. **46:** 123–134, doi:10.1111/j.1529-8817.2009.00793.x

———, and others. 2012. Nitrogen source and P_{CO_2} synergistically affect carbon allocation, growth and morphology of the coccolithophore *Emiliania huxleyi*: potential implications of ocean acidification for the carbon cycle. Glob. Change Biol. **18:** 493–503, doi:10.1111/j.1365-2486.2011.02575.x

MacIntyre, H. L., T. M. Kana, T. Anning, and R. J. Geider. 2002. Photoacclimation of photosynthesis irradiance response curves and photosynthetic pigments in microalgae and cyanobacteria. J. Phycol. **38:** 17–38, doi:10.1046/j.1529-8817.2002.00094.x

Mackinder, L., G. Wheeler, D. Schroeder, U. Riebesell, and C. Brownlee. 2010. Molecular mechanisms underlying calcification in coccolithophores. Geomicrobiol. J. **27:** 585–595, doi:10.1080/01490451003703014

Mehrbach, C., C. H. Culberson, J. E. Hawley, and R. M. Pytkowicz. 1973. Measurement of the apparent dissociation constants of carbonic acid in seawater at atmospheric pressure. Limnol. Oceanogr. **18:** 897–907, doi:10.4319/lo.1973.18.6.0897

Pierrot, D. E., E. Lewis, and D. W. R. Wallace. 2006. MS Excel program developed for CO_2 system calculations. Carbon Dioxide Information Analysis Center, Oak Ridge National Laboratory, U.S. Department of Energy, Available from http://cdiac.ornl.gov/ftp/co2sys

Raven, J. A., L. A. Ball, J. Beardall, M. Giordano, and S. C. Maberly. 2005. Algae lacking carbon concentrating mechanisms. Can. J. Bot. **83:** 879–890, doi:10.1139/b05-074

Richier, S., S. Fiorini, M.-E. Kerros, P. Von Dassow, and J.-P. Gattuso. 2011. Response of the calcifying coccolithophore *Emiliania huxleyi* to low pH/high P_{CO_2}: From physiology to molecular level. Mar. Biol. **158:** 551–560, doi:10.1007/s00227-010-1580-8

Ridgwell, A. J., I. Zondervan, J. C. Hargreaves, J. Bijma, and T. M. Lenton. 2007. Assessing the potential long-term increase of oceanic fossil fuel CO_2 uptake due to CO_2-calcification feedback. Biogeosciences **4:** 481–492, doi:10.5194/bg-4-481-2007

Riebesell, U., I. Zondervan, B. Rost, P. D. Tortell, E. Zeebe, and F. M. M. Morel. 2000. Reduced calcification in marine plankton in response to increased atmospheric CO_2. Nature **407:** 634–637, doi:10.1038/35030078

Rokitta, S. D., L. J. de Nooijer, S. Trimborn, C. de Vargas, B. Rost, and U. John. 2011. Transcriptome analyses reveal differential gene expression patterns between life-cycle stages of *Emiliania huxleyi* (Haptophyta) and reflect specialization to different ecological niches. J. Phycol. **47:** 829–838, doi:10.1111/j.1529-8817.2011.01014.x

Rost, B., S. A. Kranz, K.-U. Richter, and P. D. Tortell. 2007. Isotope disequilibrium and mass spectrometric studies of inorganic carbon acquisition by phytoplankton. Limnol. Oceanogr.: Methods **5:** 328–337, doi:10.4319/lom.2007.5.328

———, U. Riebesell, S. Burkhardt, and D. Sültemeyer. 2003. Carbon acquisition of bloom-forming marine phytoplankton. Limnol. Oceanogr. **48:** 55–67, doi:10.4319/lo.2003.48.1.0055

———, and U. Riebesell. 2004. Coccolithophores and the biological pump: Responses to environmental changes, p. 76–99. *In* H. R. Thierstein and E. B. Young [eds.], Coccolithophores—from molecular processes to global impact. Springer.

———, ———, and D. Sültemeyer. 2006. Carbon acquisition of marine phytoplankton: Effect of photoperiod length. Limnol. Oceanogr. **51:** 12–20, doi:10.4319/lo.2006.51.1.0012

Shi, D., Y. Xu, B. M. Hopkinson, and F. M. M. Morel. 2010. Effect of ocean acidification on iron availability to marine phytoplankton. Science **327:** 676–679, doi:10.1126/science.1183517

Smith, E. L. 1936. Photosynthesis in relation to light and carbon dioxide. PNAS **22:** 504–511, doi:10.1073/pnas.22.8.504

Stoll, M. H. C., K. Bakker, G. H. Nobbe, and R. R. Haese. 2001. Continuous-flow analysis of dissolved inorganic carbon content in seawater. Anal. Chem. **73:** 4111–4116, doi:10.1021/ac010303r

Suffrian, K., K. G. Schulz, M. A. Gutowska, U. Riebesell, and M. Bleich. 2011. Cellular pH measurements in *Emiliania huxleyi* reveal pronounced membrane proton permeability. New Phytol. **190:** 595–608, doi:10.1111/j.1469-8137.2010.03633.x

Sültemeyer, D., B. Klughammer, M. R. Badger, and G. D. Price. 1998. Fast induction of high-affinity HCO_3^- transport in cyanobacteria. Plant Physiol. **116:** 183–192, doi:10.1104/pp.116.1.183

Taylor, A. R., A. Chrachi, G. Wheeler, H. Goddard, and C. Brownlee. 2011. A voltage-gated H^+ channel underlying pH homeostasis in calcifying coccolithophores. PLoS Biol. **9:** e1001085, 1–14, doi:10.1371/journal.pbio.1001085

Trimborn, S., G. Langer, and B. Rost. 2007. Effect of varying calcium concentrations and light intensities on calcification and photosynthesis in *Emiliania huxleyi*. Limnol. Oceanogr. **52:** 2285–2293, doi:10.4319/lo.2007.52.5.2285

———, N. Lundholm, S. A. Thoms, K.-U. Richter, B. Krock, P. J. Hansen, and B. Rost. 2008. Inorganic carbon acquisition in potentially toxic and non-toxic diatoms: The effect of pH-induced changes in seawater carbonate chemistry. Physiol. Plant. **133:** 92–105, doi:10.1111/j.1399-3054.2007.01038.x

Tyrrell, T., and A. Merico. 2004. *Emiliania huxleyi*: Bloom observations and the conditions that induce them, p. 75–97. *In*: H. R. Thierstein and J. R. Young [eds.], Coccolithophores: From molecular processes to global impact. Springer.

Von Dassow, P., H. Ogata, I. Probert, P. Wincker, C. Da Silva, S. Audic, J.-M. Claverie, and C. De Vargas. 2009. Transcriptome analysis of functional differentiation between haploid and diploid cells of *Emiliania huxleyi*, a globally significant photosynthetic calcifying cell. Genome Biol. **10:** R114, doi:10.1186/gb-2009-10-10-r114

Weiss, R. F. 1970. The solubility of nitrogen, oxygen and argon in water and seawater. Deep-Sea Res. **17:** 721–735, doi:10.1016/0011-7471(70)90037-9

Zondervan, I., B. Rost, and U. Riebesell. 2002. Effect of CO_2 concentration on the PIC : POC ratio in the coccolithophore *Emiliania huxleyi* grown under light-limiting conditions and different daylengths. JEMBE **272:** 55–70, doi:10.1016/S0022-0981(02)00037-0

———, R. E. Zeebe, B. Rost, and U. Riebesell. 2001. Decreasing marine biogenic calcification: A negative feedback on rising atmospheric P_{CO_2}. Glob. Biogeochem. Cycles **15:** 507–516.

Associate Editor: Robert R. Bidigare

Received: 11 October 2011
Accepted: 03 January 2012
Amended: 10 January 2012